STM JOURNALS

Research & Reviews: Journal of
Space Science & Technology

https://journals.stmjournals.com/rrjosst

ISSN: 2321-2837 (Online)
ISSN: 2321-6506 (Print)
Volume 13, Issue 3, 2024
September–December
DOI (Journal): 10.37591/RRJoSST

Research RRJoSST

Analysis of the Wave Function of Perturbed Ionospheric Waves for Communication Signals

Aasim Sultan Khoja[1,*], Purvee Bhardwaj[2]

Abstract

Our daily communications and navigational systems rely on the ionospheric conditions, and this sensitive region of the atmosphere is traversed and governed by radio and global positioning system (GPS) signals which broadcast on bouncing off the ionosphere to reach their destinations. All the communication signals can be interfered with modifications because of the changes in the ionosphere's density and its composition so that large percentage of the free electrons in the ionosphere affect radio wave signal propagation and disturb our communication signal. The ionosphere's free electrons oscillate in response to high-frequency radio waves, which cause them to radiate energy back down at the same frequency. This essentially makes the radio wave to return to the earth. The wave function study of the perturbed ionospheric waves is a mathematical description that explains or describes disturbances in the ionosphere. It typically involves solving complex equations to model the behavior of perturbed ionospheric waves, considering factors like electron density variations and magnetic field interactions. The specific form of the wave function depends on the type of perturbation and the underlying physics involved.

Keywords: Ionospheric storm, solar activity, airport communication signal, ionospheric critical frequency, sudden ionospheric disturbances

INTRODUCTION

Ionospheric storms refer to the highly perturbed conditions of the ionospheric layers, particularly the F layer caused due to the highly variable and magnetospheric energy inputs into the earth's ionosphere. Ionospheric storms, according to scientists, are caused by solar particle radiation. The solar eruption's ultraviolet light waves travel at a faster speed than the particles it emits. This would explain the roughly 18-hour time delay between an ionospheric storm and sudden ionospheric disturbances. An ionospheric storm connected to sunspot activity can start anywhere between two days before an active sunspot crosses the sun's central meridian and 4 days after it. Solar activity is closely linked to magnetic fields, which are thought to originate from a dynamo action within the sun [1]. The sun is a magnetic variable star that can fluctuate on timescales ranging from a fraction of a second to billions of years.

***Author for Correspondence**
Aasim Sultan Khoja
E-mail: aasimkhaja@rediffmail.com

[1]Research Scholar, Department of Physics, Rabindranath Tagore University, Raisen, Madya Pradesh, India
[2]Dean, Department of Physics, Rabindranath Tagore University, Raisen, Madya Pradesh, India

Received Date: October 16, 2024
Accepted Date: October 23, 2024
Published Date: October 30, 2024

Citation: Aasim Sultan Khoja, Purvee Bhardwaj. Analysis of the Wave Function of Perturbed Ionospheric Waves for Communication Signals. Research & Reviews: Journal of Space Science & Technology. 2024; 13(3): 13–20p.

Moreover, at times it is also witnessed that when active sunspots have passed through the sun's center no ionospheric storms are created [2]. The storms in the ionosphere may strike quickly into the atmosphere. Ionospheric storms primarily cause a turbulent ionosphere and extremely unpredictable radio wave propagation. Particularly for the F2 layer, critical frequencies are lowered than usual due to these storms. Ion density is decreased in the upper F2 layer because of this. Except for severe disturbances, lower levels do not suffer much. Ionospheric storms have the practical consequence of decreasing the range of frequencies that may be utilized for communications signals in comparison

to normal conditions and the communication remains confined to the lower frequencies affecting long distance communication [3]. German astronomer Samuel Heinrich Schwabe discovered the solar cycle through his observations of sunspots. Swiss astronomer Rudolf Wolf reconstructed solar activity back to the 17th century. International Civil Aviation Organization (ICAO) regulations require air traffic control towers to possess such signal lamps. The signal lamp has a focused bright beam and can emit three different colors: red, white and green. These colors may be flashed or steady and have different meanings to aircraft in flight or on the ground [4].

MATERIALS AND METHODS

The wave function for radio waves can be described mathematically by the sinusoidal wave equation, the wave function (E) for an electromagnetic radio wave can be represented as

$$[E\ (x,\ t) = E_0 \cos\ (kx - \omega t)] \tag{1}$$

where, $E\ (x,\ t)$ is electric field at position (x) and time (t), E_0 is the amplitude of the electric field, k is the wave number, related to the wavelength, ω is the angular frequency. This equation represents a propagating wave with a specific frequency and wavelength. In the context of radio waves, variations and complexities may arise based on the specific characteristics of the medium through which the wave is propagating and any potential perturbations or interactions it experiences [5].

Now, to measure the impact of ionospheric storms on communication signals, seven very low frequency (VLF) stations' data and nearly 8000 airports' communication signal data are examined [6]. The communication signal strength is measured by power of the signal collected by the antenna which are usually expressed in dBm.

$$P = \frac{E_{RMS}^2}{R} \tag{2}$$

Typically, this is converted to decibels relative to dBm.

$$L_{dBm} = 10log_{10}\left(\frac{P}{0.001W}\right) \tag{3}$$

RESULTS

The ionospheric storms occur due to solar wind generations and some coronal mass ejection (CME) events which are observed during the observed period on 06 September 2022 06:00:00 to 06 September18:00:00. The vertical dashed lines represent the CME duration in the plotted graph in Figure 1 [7]. Present measurements data is sampled at Δt = 3600 s in the last step of the analysis so that comparison with the communication signal frequency could be performed by using the data with a similar sampling time. Because of the strong statistical nature of the analysis and the robustness of the airport signal strength database, no pre- processing of the data was necessary [8]. On the flip side, the ionosphere's critical frequency was observed through radio propagation and the limiting frequency at below by which a wave function is reflected and penetrates through into an ionospheric layer. At critical frequency below the incidence, the wave function is reflected and penetrates through an ionospheric layer. Sudden ionospheric disturbances (SIDs) are caused by solar flare enhanced X-rays in the 1 to 10 Å (angstrom) range [9]. Solar flares can produce large increases of ionization in the D-region of the ionosphere over the daylit hemisphere of the Earth Critical Frequency shows variations with solar activity and atmospheric perturbation in addition to angle between the radio waves and antenna. The presence of the critical frequency is the result of electron limitation, the inadequacy of the existing number of free electrons to support reflection at higher frequencies [10]. It is the highest magnitude of frequency of ionosphere above which the waves penetrate the ionosphere and below which the signals get bounced back from the ionosphere. It is denoted by "fc". Its value is not fixed, and it depends upon the electron density of the ionosphere. Critical frequency can be computed with the electron density given by:

$$f_c = 9\sqrt{Nmax} \tag{4}$$

where, $Nmax$ is maximum electron density per m^3 and f_c is in Hz.

DISCUSSION

In Figure 1, the variation in the worldwide airport communication data in terms of frequency in the range of -200 to 1400 Hz, on 06 September 2022 06:00:00 to 06 September 18:00:00 is reported [11–15]. Communication signal frequency can be investigated to analyze the disturbances in the communication system due to ionospheric disturbances. To study the ionospheric wave function of critical frequency it is correlated with worldwide airport communication signal. The main advantage of using correlation methods is the ability to extract frequency information from a complex time series using similar day temporal window. Communication signal frequency transforms a signal into a Fourier series of coefficients which is associated with ionospheric critical frequency [16–20]. SID offers an alternate method to analyze the effect of solar wind on the ionosphere and disturb the communication signal. Figure 2 clearly shows that the critical frequency is at its peak during the daytime on 06 September 2022 [21–25]. It is also clear in this graph that at the time of solar storm of class 1 critical frequency may increase in the ionosphere but its effect in the worldwide airport frequency maximum goes up to 1300 Hz, which is extremely value in terms of general frequency trend which lie in between 300 and 900 Hz. Thus, the value of critical frequency in Figure 3 increases in the morning time on 06 September 2022 and solar storm of class 4 also occurs in the morning time around 06:00 am [26]. But Figure 4 shows another station data of ionospheric critical frequency value with no changes due to solar storm and due to this station, it seems that there was no effect on the airport communication signal. Figure 3 shows the NRK VLF stations of SID monitoring system indicating the variations of critical frequency due to various solar storms. The maximum value of critical frequency in Figure 5 is falling between two solar storms of different classes; such types of modulated waves may also affect the communication signal [27].

Figure 6 shows completely different behavior from the normal behavior of ionospheric critical frequency, despite being a solar storm graph it has not shown maximum value of critical frequency on 06 September 2022. Whatever the maximum value is obtained is outside the defined limits of the selected day. In the same sequence, Figure 7 shows the normal trend, or sinusoidal waveforms have been generated due to solar storm and the periodical variation of critical frequency is observed. The trend of critical frequency and airport frequency are almost similar at this station, so that wave function in terms of critical frequency may satisfy. In Figure 8, another SID station data is shown and the maximum value of critical frequency occurs in the daytime on 06 September 2022, when the solar storm of class 1 reaches the earth environment.

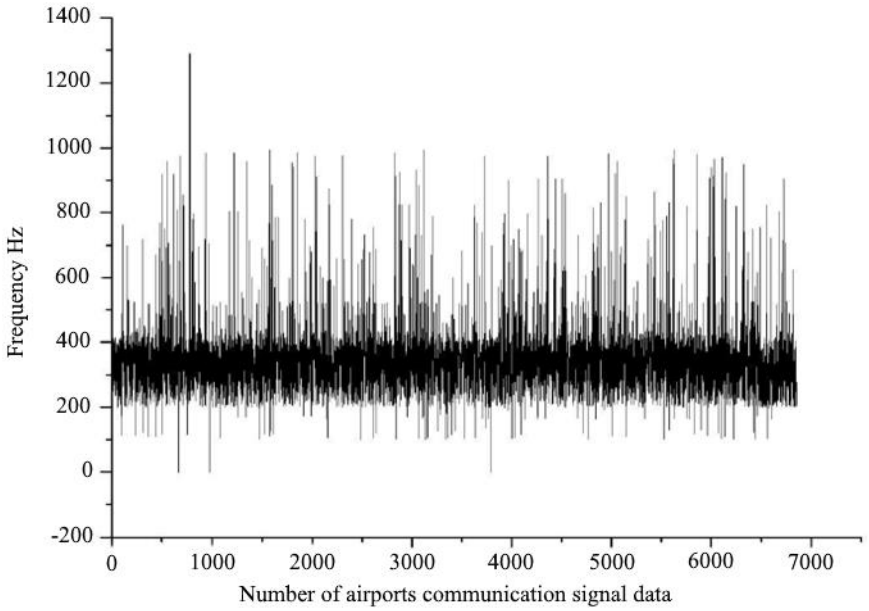

Figure 1. Number of airports communication signal data.

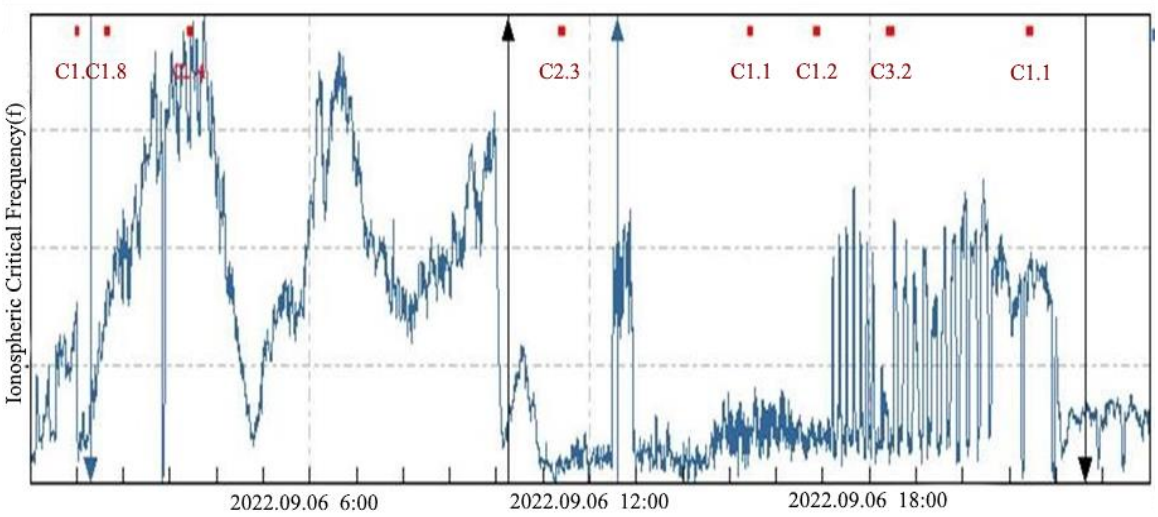

Figure 2. NAU Roswell meteor very low frequency (VLF) station for critical frequency (*f*).

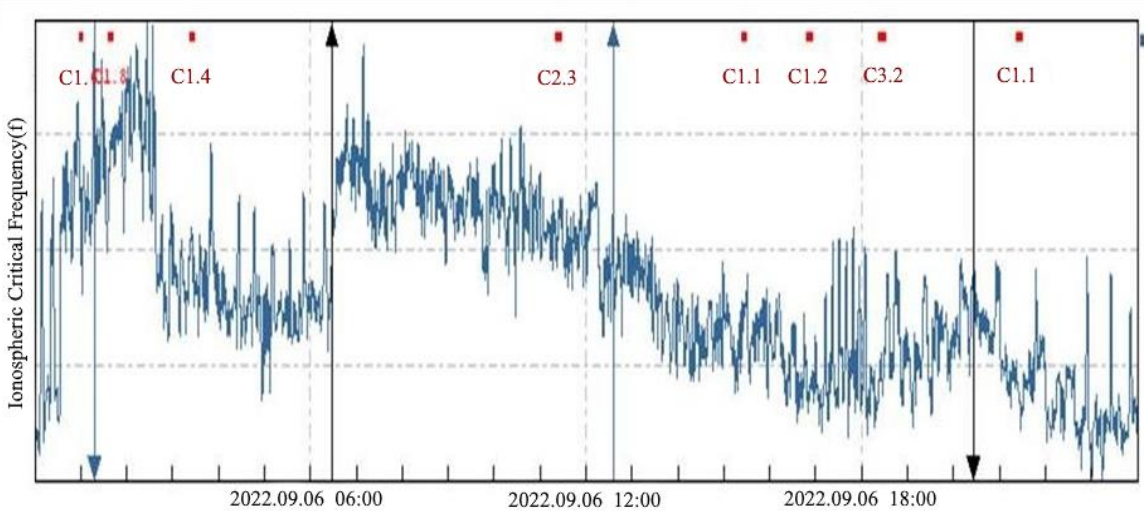

Figure 3. NRK Roswell meteor very low frequency (VLF) station for critical frequency (*f*) due to various solar storms.

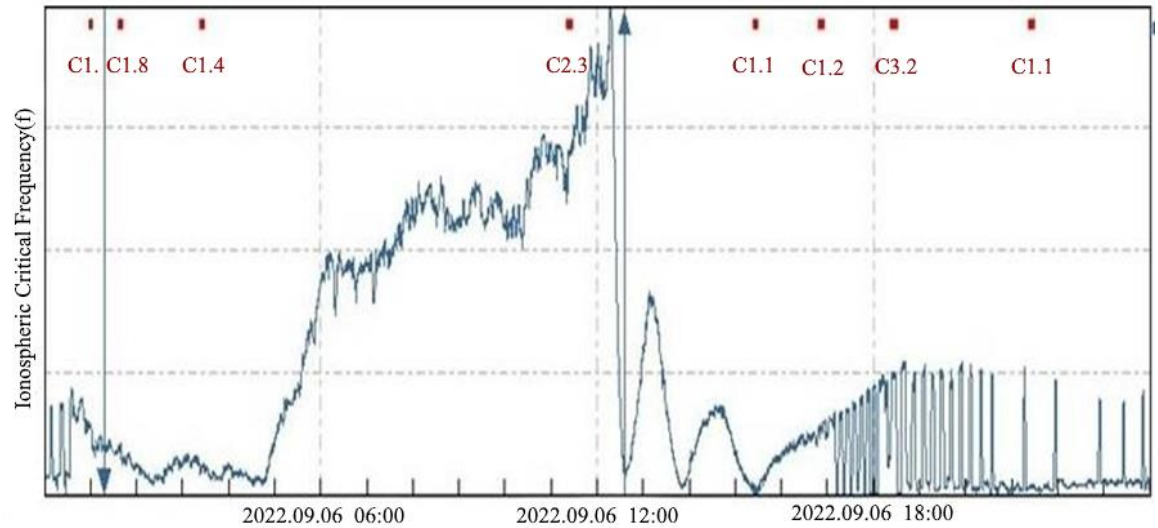

Figure 4. NRK Roswell meteor very low frequency (VLF) station for critical frequency (*f*).

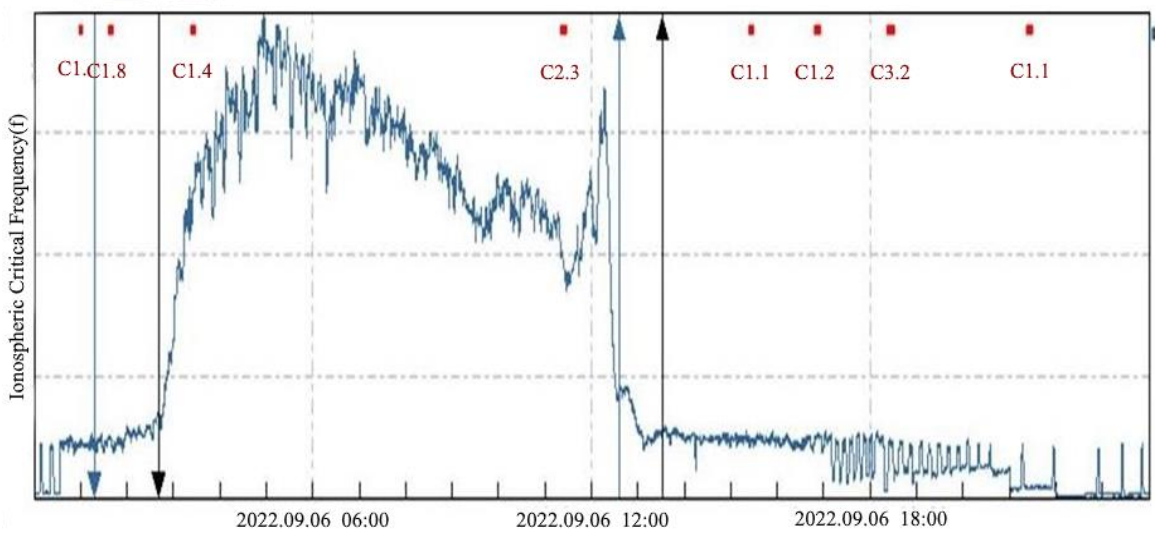

Figure 5. NRK Roswell meteor very low frequency (VLF) station for critical frequency (*f*): Maximum value.

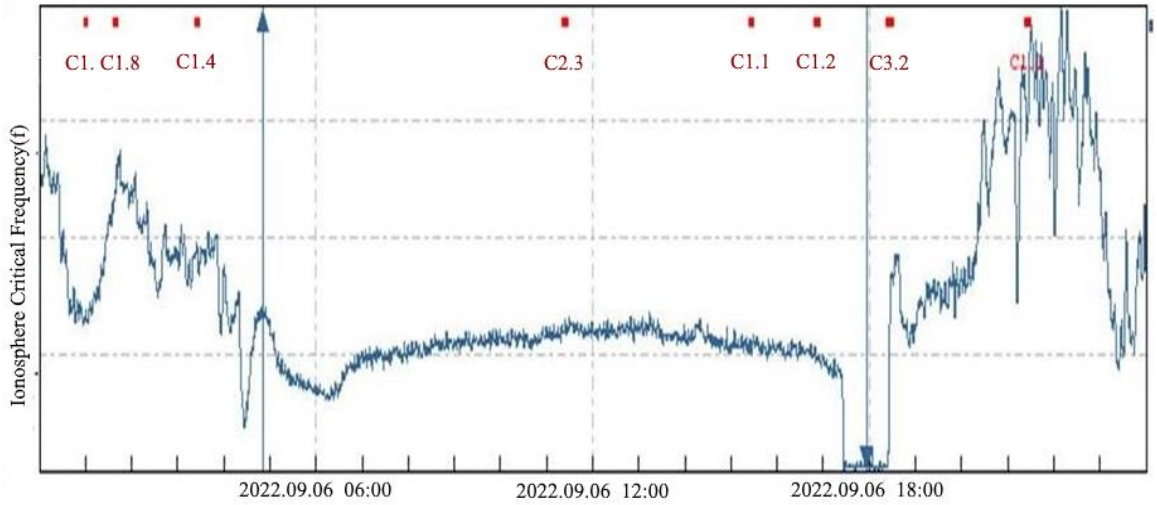

Figure 6. Comparison between normal and modulated wave.

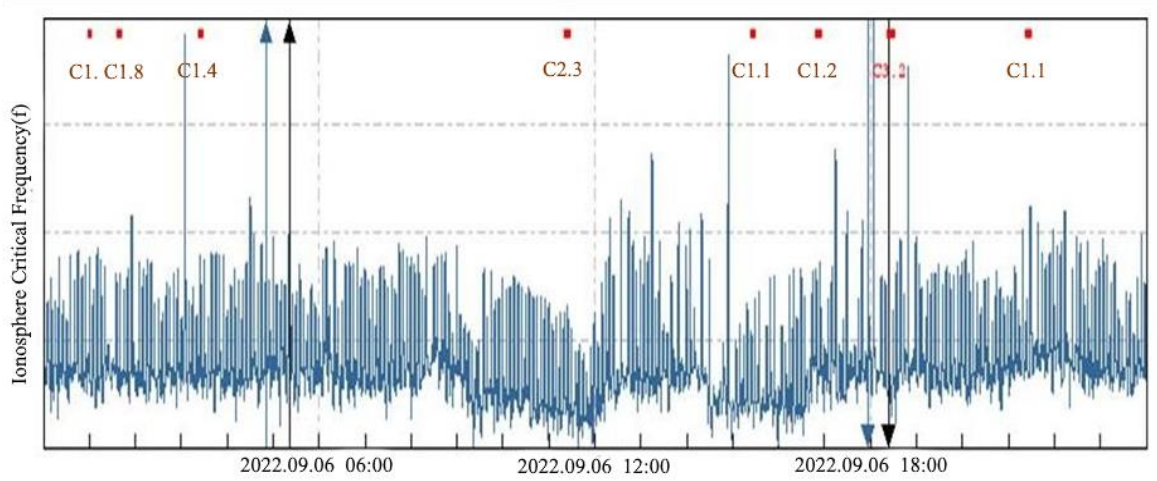

Figure 7. Periodical variation of critical frequency.

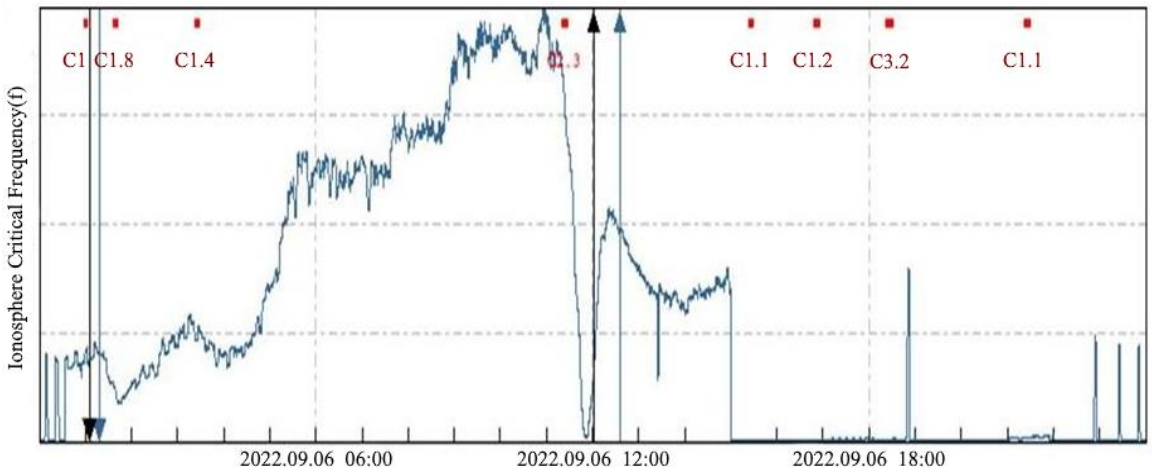

Figure 8. Another SID station data.

CONCLUSION

The ionosphere will be recognized as a helpful instrument for long-distance radio communication in the high frequency band considering the anticipated outcomes. When very high frequency (VHF) waves are used as a communication signal from a satellite or space probe to Earth, the situation is entirely different. The ionosphere works as a degrading medium and affects the navigation performance of communication signal systems; the key frequency of the F2 area is employed to avoid their reflection back to space-based systems. Numerous radio propagation effects exist, contingent on the type of medium required for the signal to go from Earth to space. Ionosphere scintillation, Doppler frequency shift, polarization, absorption, refraction, and propagation time delay are a few examples of these. Range error arises in tracking and navigation applications from two sources: a decrease in communication signal frequency and an increase in path length brought on by refraction-induced radio wave bending. The phenomenon known as scintillation is caused by variations in the signal strength and phase of a radio wave passing through ionospheric medium. Enhancement and fading around the medium level are caused by ionospheric scintillation when the radio signal passes through the disturbed ionospheric area. A band encircling the geomagnetic equator and sub-auroral to polar latitudes are two regions of the world that are severely plagued by scintillation. Therefore, propagation lines that cross the auroral and equatorial ionosphere are more likely to cause deterioration of earth-space communication signal linkages. This impact is amplified by the worldwide distribution of scintillation at the L band (1.5 GHz) during the solar maximum and minimum dates. The results depict that the intensity of scintillation rises with solar activity, and it seems more severe close to the magnetic equator than it exists in subaerial to polar areas. Here are a few consequences for earth-space communication propagation systems caused by ionospheric scintillation:

1. In satellite communication systems, message errors occur when the depth of fading caused by scintillation surpasses the fading margin of the receiving system.
2. Phase scintillation can result in a decrease of communication signal strength in the Nav-Aids system, while amplitude scintillation can result in cycle skips and data loss.
3. Scintillation in radar systems can cause false signals or interfere with radar target characteristics.
4. The aircraft's downlink is the most path-sensitive to signal amplitude due to power constraints and limited antenna gain.
5. In high-speed digital communication systems, the fading depth approaches a value below system sensitivity and the fading time is larger than the pulse length.

REFERENCES

1. Chowdhury S, Kundu S, Ghosh S, Sasmal S, Brundell J, Chakrabarti SK. Statistical study of global lightning activity and thunderstorm-induced gravity waves in the ionosphere using WWLLN and GNSS-TEC. J Geophys Res Space Phys. 2023; 128 (1): e2022JA030516. doi: 10.1029/2022JA030516.

2. Cesaroni C, Spogli L, Aragon-Angel A, Fiocca M, Dear V, De Franecschi G, Romano V. Neural network-based model for global total electron content forecasting. J Space Weather Space Clim. 2020; 10: Article 11. doi: 10.1051/swsc/2020013.
3. Bruno R, Carbone V. The solar wind as a turbulence laboratory. Living Rev Sol Phys. 2013; 10: Article 2.
4. Telloni D, Carbone F, Antonucci E, Bruno R, Grimani C, Villante U, Giordano S, Mancuso S, Zangrilli L. Study of the influence of the solar wind energy on the geomagnetic activity for space weather science. Astrophys J. 2020; 896 (2): 149.
5. Castillo Y, Pais MA, Fernandes J, et al. Relating 27-day averages of solar, interplanetary medium parameters, and geomagnetic activity proxies in solar cycle 24. Sol Phys. 2021; 296: 115.doi: 10.1007/s11207-021-01856-8.
6. Berdermann J, Kriegel M, Banys D, Heymann F, Hoque MM, Wilken V, Borries C, Heßelbarth A, Jakowski N. Ionospheric response to the X9.3 flare on 6 September 2017 and its implication for navigation services over Europe. Space Weather. 2018; 16 (10): 1604–1615. doi: 10.1029/2018SW001933.
7. Berdermann J, Sato H, Kriegel TM, Fujiwara T, Tsujii T. Effects of equatorial ionospheric scintillation for GNSS based positioning in aviation. In: 2020 European Navigation Conference (ENC), Dresden, Germany, November 23–24, 2020. pp. 1–8, doi: 10.23919/ENC48637.2020.9317407.
8. Beedle JMH, Rura CE, Simpson DG, Cohen HI, Moraes Filho VP, Uritsky VM. A user's guide to the magnetically connected space weather system: a brief review. Front Astron Space Sci. 2022; 8: 253.
9. Bruno R, Carbone V. Turbulence in the Solar Wind. 1st edition. Lecture Notes in Physics 928. New York, NY, USA: Springer International Publishing; 2016.
10. Burton RK, McPherron RL, Russell CT. An empirical relationship between interplanetary conditions and *Dst*. J Geophys Res (1896–1977). 1975; 80: 4204–4214.
11. Buzulukova N, editor. Extreme Events in Geospace. Amsterdam, The Netherlands: Elsevier; 2018.
12. Cander LR, Mihajlovic SJ. Forecasting ionospheric structure during the great geomagnetic storms. J Geophys Res Space Phys. 1998; 103: 391–398.
13. Cannon P, Angling M, Barclay L, Curry C, Dyer C, Edwards R, Underwood C. Extreme Space Weather: Impacts on Engineered Systems and Infrastructure. London, UK: Royal Academy of Engineering; 2013. Available at https://raeng.org.uk/media/lz2fs5ql/space_weather_full_report_final.pdf
14. Castillo Y, Pais MA, Fernandes J, Ribeiro P, Morozova AL, Pinheiro FJG. Relating 27-day averages of solar, interplanetary medium parameters, and geomagnetic activity proxies in solar cycle 24. Sol Phys. 2021; 296: 115.
15. Koskinen HEJ, Baker DN, Balogh A, Gombosi T, Veronig A, Von Steiger R. Achievements and challenges in the science of space weather. Space Sci Rev. 2017; 212: 1137–1157.
16. Cesaroni C, Spogli L, Franceschi GD, Damaceno JG, Grzesiak M, Vani B, Monico JFG, Romano V, Alfonsi L, Cafaro M. A measure of ionospheric irregularities: zonal velocity and its implications for L-band scintillation at low-latitudes. Earth Planet Phys. 2021; 5 (5): 450–461. doi: 10.26464/epp2021042.
17. Chou M-Y, Cherniak I, Lin CCH, Pedatella NM. The persistent ionospheric responses over Japan after the impact of the 2011 Tohoku earthquake. Space Weather. 2020; 18: e2019SW002302. doi: 10.1029/2019SW002302.
18. Ishii M, Berdermann J, Forte B, Hapgood M, Bisi MM, Romano MM. Space weather impact on radio communication and navigation. Adv Space Res. 2024. In press. doi: 10.1016/j.asr.2024.01.043.
19. Consolini G. Self-organized criticality: a new paradigm for magnetotail dynamics. Fractals. 2002; 10: 275–283.
20. Consolini G, De Michelis P, Tozzi R. On the Earth's magnetospheric dynamics: nonequilibrium evolution and the fluctuation theorem. J Geophys Res Space Phys. 2008; 113: A8.
21. Dellinger JH. Sudden ionospheric disturbances. Terr Magn Atmos Electr. 1937; 42 (1): 49–53. doi: 10.1029/TE042i001p00049.

22. Demirkol MK, Inan US, Bell TF, Kanekal SG, Wilkinson DC. Ionospheric effects of relativistic electron enhancement events. Geophys Res Lett. 1999; 26 (23): 3557–3560. doi: 10.1029/1999GL010686.
23. Dungey JW. Interplanetary magnetic field and the auroral zones. Phys Rev Lett. 1961; 6 (2): 47. doi: 10.1103/PhysRevLett.6.47.
24. Fallows RA, Bisi MM, Forte B, Ulich T, Konovalenko AA, Mann G, Vocks C. Separating nightside interplanetary and ionospheric scintillation with LOFAR. Astrophys J Lett. 2016; 828 (1): L7.
25. Fallows RA, Iwai K, Jackson BV, Zhang P, Bisi MM, Zucca P. Application of novel interplanetary scintillation visualizations using LOFAR: a case study of merged CMEs from September 2017. Adv Space Res. 2023; 72 (12): 5311–5327. doi: 10.1016/j.asr.2022.08.076.
26. Farge M. Wavelet transforms and their applications to turbulence. Annu Rev Fluid Mech. 1992; 24: 395–458.
27. Fishing News. DECCA: More Gear Lost. Fishing News (UK) London, Arthur J Heighway Publications Ltd., Issue dated 16 December 1983.

